

Supporting Information

Self-assembly of Hyaluronic Acid-mediated Tumor- targeting Theranostics Nanoparticles

Xiaoxuan Zhou,^{1, §} Chengbin He,^{1, §} Min Liu,¹ Qingqing Chen,¹ Lingjie Zhang,¹
Xiaodan Xu,² Hongxia Xu,² Yue Qian,¹ Feidan Yu,¹ Yan Wu,¹ Yuxin Han,¹ Bing
Xiao,^{2*} Jianbin Tang,^{2*} Hongjie Hu^{1*}

¹ Department of Radiology, Sir Run Run Shaw Hospital (SRRSH) of School of
Medicine, Zhejiang University, Hangzhou, Zhejiang, 310016, China.

² Key Laboratory of Biomass Chemical Engineering of Ministry of Education, Center
for Bionanoengineering, and College of Chemical and Biological Engineering,
Zhejiang University, Hangzhou, Zhejiang, 310027, China.

*Corresponding Author: xiaobingphd@zju.edu.cn, jianbin@zju.edu.cn,
hongjiehu@zju.edu.cn

§These authors equally contributed to this work.

Synthesis of Cy5.5-labeled HMDN

The 5 mL HMDN solution (3mg mL⁻¹) was mixed with 300 µL Cy5.5-NHS (1 mg mL⁻¹), stirred for 12 h in the dark, and purified by ultrafiltration (molecularweight cut-off: 3 K Da).

***In vivo* PTT**

For *in vitro* photothermal experiment, temperature change of HMDN under four laser irradiation on/off cycles was recored by a photothermal imager. Besides, the temperature changes of HMDN at different concentrations (0.75, 0.5, 0.25, 0.125 mg mL⁻¹) under laser irradiation (808 nm, 2 W cm⁻², 5 min), were recorded every ten seconds.

Colloidal and Optical Stability Measuremen

For the observation of colloidal stabilization, 1 mg mL⁻¹ of HMDN were dispersed in DI water, PBS, RPMI-1640 culture medium, and normal saline, respectively. Hydrodynamic diameters were monitored throughout a period of 7 days.

Statistical analysis

Quantitative data were expressed as the mean ± standard deviation, as discribed in the figure legends. Statistical analysis was conducted using a Student's t-test. Significant differences were estimated by * $p < 0.05$, ** $p < 0.01$, *** $p < 0.001$.

Supporting data

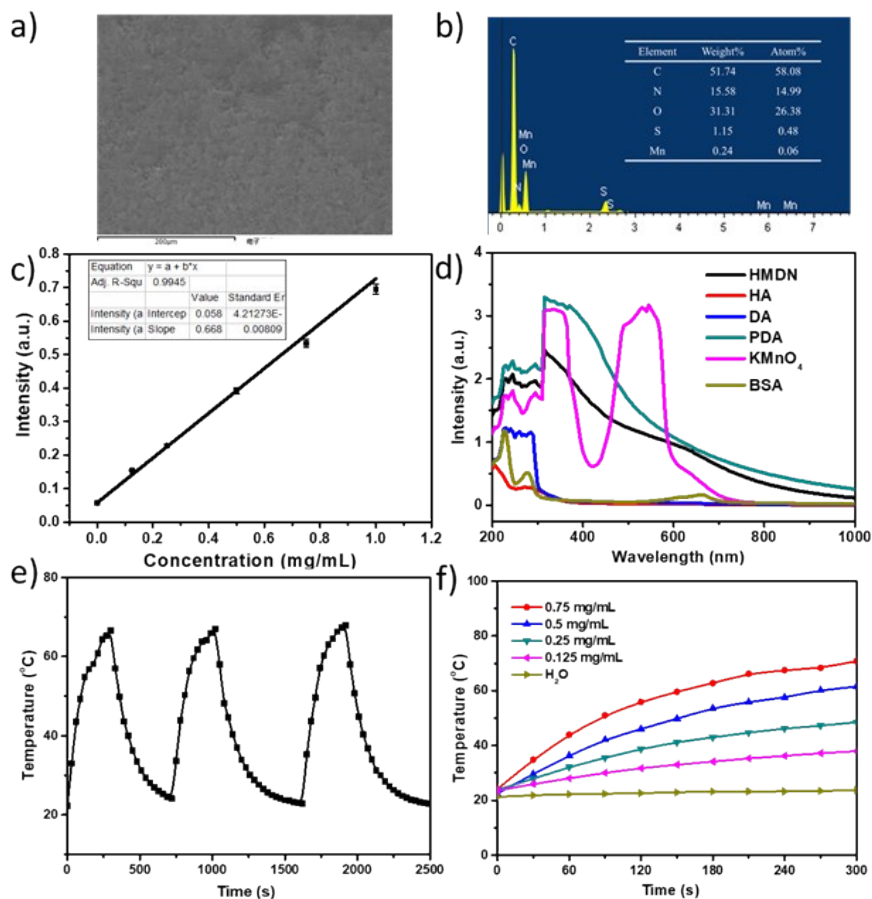


Figure S1. (a) The EDS data of the HMDN. (b) UV-vis absorption spectra of HMDN, HA, DA, PDA, KMnO₄ and BSA solutions. (c) The intensity at 808 nm as a function of HMDN concentration. (d) Absorption spectra of HMDN, HA, DA, PDA, BSA and KMnO₄ solutions. (e) Changes in temperature of the HMDN upon laser irradiation (808 nm, 2.0 W cm⁻², and 5 min) for three laser on/off cycles. (f) Photothermal heating profile of the HMDN at different concentration under laser irradiation (808 nm, 2.0 W cm⁻², and 5 min).

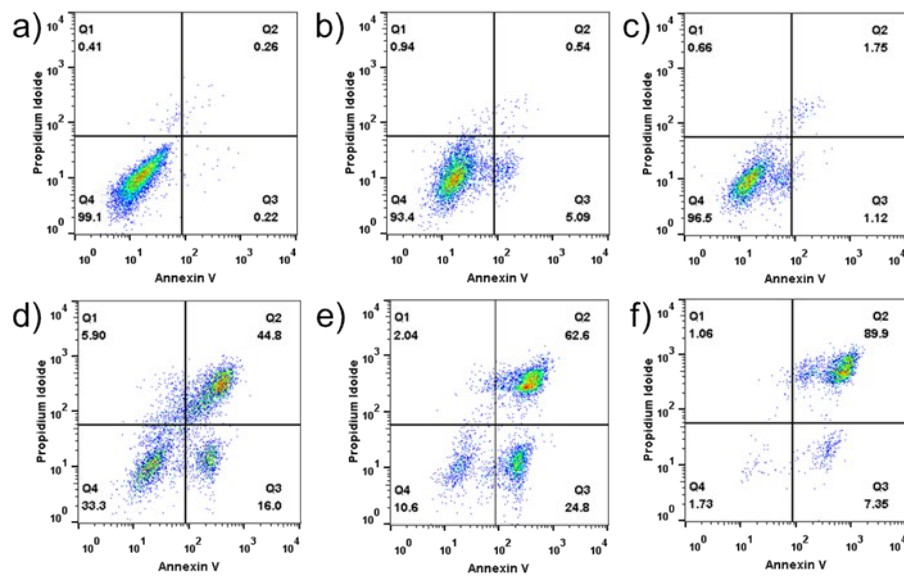


Figure S2. Flow cytometry-based apoptosis of 4T1 cells. (a) PBS only, (b) Laser only, (c) HMDN only (55 μM Mn), (d) HMDN with free HA under laser, (e) MDN under laser, (f) HMDN under laser (808 nm, 2W cm^{-2} , 5 min).

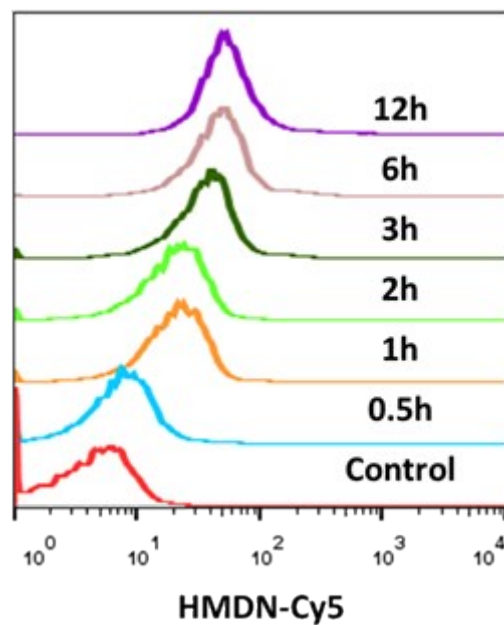


Figure S3. Flow cytometry analysis of cellular uptake of Cy5.5-labeled HMDN (55 μM Mn) at different times.

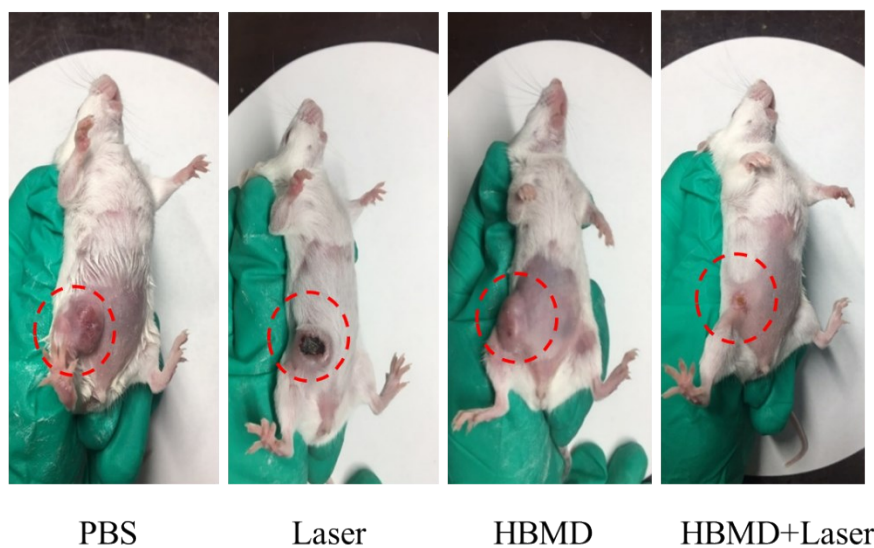


Figure S4. Representative photographs of mice bearing orthotropic 4T1 tumors after different treatments (as indicated) taken on day 15.

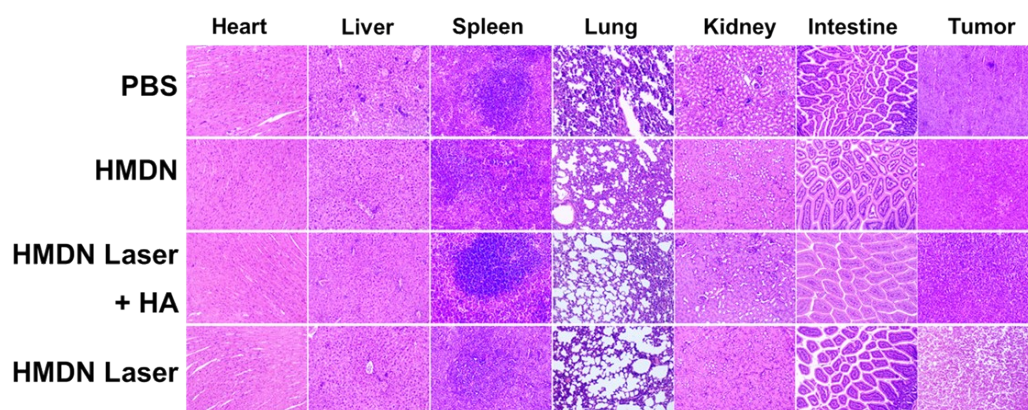


Figure S5. H&E-stained images of the major organs from four different treatment groups (PBS, HMDN, HMDN plus HA with PTT 5 min, and HMDN with PTT 5 min) mice after 15 days ($0.02 \text{ mmol kg}^{-1} \text{ Mn}$, 808 nm , 2 W cm^{-2}). Scale bar $200 \mu\text{m}$, magnification $\times 200$.

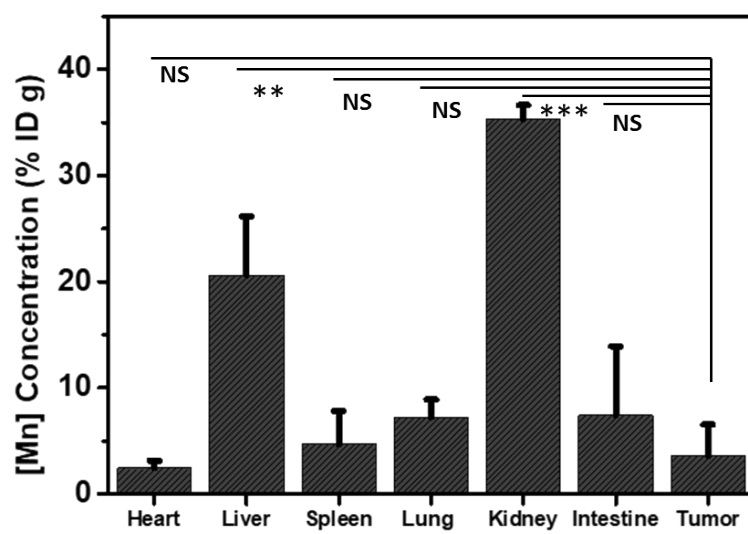


Figure S6. One day after administration, Mn content in main organs and tumor of 4T1 orthotopic tumor-bearing mice ($0.02 \text{ mmol kg}^{-1} \text{ Mn}$).